

LETTER TO THE EDITOR

Suzaku, Chandra, and XMM-Newton Analysis of Abell 2204: The Galaxy Cluster Gas Temperature Profile from 10 kpc to 1800 kpc.

T. H. Reiprich¹, D. S. Hudson¹, Y.-Y. Zhang¹, K. Sato², Y. Ishisaki³, A. Hoshino³, T. Ohashi³, N. Ota^{4,5}, and Y. Fujita⁶

¹ Argelander Institute for Astronomy, Bonn University, Auf dem Hügel 71, D-53121 Bonn, Germany
e-mail: thomas@reiprich.net

² Graduate School of Natural Science and Technology, Kanazawa University, Kakuma, Kanazawa, Ishikawa, 920-1192, Japan

³ Department of Physics, Tokyo Metropolitan University, 1-1 Minami-Osawa, Hachioji, Tokyo 192-0397, Japan

⁴ Institute of Space and Astronautical Science (ISAS/JAXA), 3-1-1 Yoshinodai, Sagami-hara, Kanagawa 229-8510, Japan

⁵ Max-Planck-Institut für extraterrestrische Physik, 85748 Garching, Germany

⁶ Department of Earth and Space Science, Graduate School of Science, Osaka University, Toyonaka, Osaka 560-0043, Japan

Received 2008

ABSTRACT

Context. Measurements of intracluster gas temperatures out to large radii, where much of the galaxy cluster mass resides, are important for the use of clusters for precision cosmology and for studies of cluster physics. Previous attempts to measure robust temperatures at cluster virial radii failed.

Aims. The goal of this work is to measure the temperature profile of the very relaxed symmetric galaxy cluster Abell 2204 out to large radii, possibly reaching the virial radius.

Methods. Taking advantage of its low particle background due to its low-Earth orbit, *Suzaku* data are used to measure the outer temperature profile of Abell 2204. These data are combined with *Chandra* and *XMM-Newton* data of the same cluster in order to make the connection to the inner regions, unresolved by *Suzaku*, and to determine the smearing due to *Suzaku*'s point-spread-function.

Results. The temperature profile of Abell 2204 is determined from ~ 10 kpc to ~ 1800 kpc, close to an estimate of r_{200} (the approximation to the virial radius). The temperature rises steeply from below 4 keV in the very center up to more than 8 keV in the intermediate range and then decreases again to about 4 keV at the largest radii. Varying the measured particle background normalization artificially by $\pm 10\%$ does not change the results significantly. Predictions for outer temperature profiles based on hydrodynamic simulations show good agreement. In particular, we find the observed temperature profile to be slightly steeper but consistent with a drop of a factor of 0.6 from $0.3 r_{200}$ to r_{200} , as predicted by simulations.

Conclusions. Intracluster gas temperature measurements up to the virial radius seem feasible with *Suzaku*, when a careful analysis of the different background components and the effects of the point-spread-function is performed. Such measurements now need to be performed for a statistical sample of clusters. The result obtained here indicates that numerical simulations capture the intracluster gas physics well in cluster outskirts.

Key words. X-rays: galaxies: clusters – galaxies: clusters: individuals: Abell 2204

1. Introduction

Cosmologically, the most important parameter of galaxy clusters is their total gravitational mass. X-rays offer an attractive way to determine this mass through measurements of the intracluster gas temperature and density structures. X-rays are also a unique tool to study the physics of the hot cluster gas, e.g., gas temperature profiles allow constraints on (the suppression of) heat conduction. Consequently, constraining cluster temperature profiles has been the subject of many (partially contradictory) works in the recent past (e.g., Fukazawa 1997; Markevitch et al. 1998; Irwin et al. 1999; White 2000; Irwin & Bregman 2000; Allen et al. 2001; De Grandi & Molendi 2002; Zhang et al. 2004; Vikhlinin et al. 2005; Arnaud et al. 2005; Kotov & Vikhlinin 2005; Piffaretti et al. 2005; Hudson & Reiprich 2006; Pratt et al. 2007; Snowden et al. 2008; Leccardi & Molendi 2008).

Unfortunately, making the aforementioned measurements is quite challenging in outer cluster regions. Even with *XMM-*

Newton and *Chandra* it is very difficult to determine temperature profiles reliably out to more than about 1/2 the cluster virial radius, r_{vir} (see the references above but also Solovyeva et al. 2007, for a different view). So, only about 1/8 of the cluster volume is actually probed. The primary reason is not insufficient collecting area or spectral resolution of current instruments: the limiting factor is the high particle background. Here, the X-ray CCDs onboard *Suzaku* come into play. Owing to its low-Earth orbit and short focal length, the background is much lower and more stable than for *Chandra* and *XMM-Newton* (Mitsuda et al. 2007), making *Suzaku* a very promising instrument for finally settling the cluster temperature profile debate. And indeed, some of us succeeded recently in measuring the temperature and metal abundance in the outskirts of the merging clusters A399/A401 (Fujita et al. 2008). In this Letter, we go one step further and confirm this great prospect also for outer cluster regions whose emissivity is not enhanced by merging activity and determine the temperature profile of the regular cluster Abell 2204 out to ~ 1800 kpc with *Suzaku*. This radius is close to an estimate of r_{200} ; i.e., the radius within which the mean total density equals

200 times the critical density, often used as approximation to the virial radius.

Throughout, we assume $\Omega_m = 0.3$, $\Omega_\Lambda = 0.7$, and $H_0 = 71$ km/s/Mpc; i.e., at the redshift of Abell 2204 ($z = 0.1523$), $1' = 157$ kpc.

2. Observations, Reduction, Analysis

2.1. *Chandra* and *XMM-Newton* data

Abell 2204 was analyzed with *Chandra* as part of the *HIFLUGCS* (Reiprich & Böhringer 2002) follow-up. The reduction and analysis are similar to those outlined in Hudson et al. (2006). The total clean exposure of the two archival observations is 18.6 ks. Further details are described in Hudson et al. (in prep.).

The *XMM-Newton* analysis of Abell 2204 is published (Zhang et al. 2008). Extrapolating the mass profile using the published gas density and temperature profile, we found $r_{200} = 11.75' = 1840$ kpc.

2.2. *Suzaku* data

Abell 2204 was observed with *Suzaku* on September 17–18, 2006. We started from the cleaned event files (processing version 1.2.2.3) and reran the `ftools xisputpixelquality` and `xispi`, using `HEASoft 6.2` and `CALDB 070409`. Using `xselect`, the event files were further filtered by applying the criteria `STATUS=0:65535`, `COR>6`, and `ELV>10`. The good exposure amounts to about 50 ks for each of the four XIS using both 3x3 and 5x5 editing modes. Figure 1 (left) shows the combined image and the regions selected for spectral analysis.

The widths of the annuli were chosen to be about twice as large as the half power diameter of the point-spread-function (PSF). Combined spectra were extracted using the filtered 3x3 and 5x5 editing mode events files. Using four regions from each of the four detectors, this resulted in 16 spectra total from the source observation. The spectra were grouped to have at least 50 counts in each energy channel.

We checked the spectra for contamination by solar wind charge exchange emission. The ACE SWEPAM proton flux was less than 6×10^8 protons/s/cm² during the observation. Therefore, no strong flaring is expected (Fujimoto et al. 2007). Moreover, we checked the soft band (<2 keV) XIS-1 lightcurve of the local background region (annulus 4) and did not find any indication of flaring.

Response files were created with `xisrmfgen` and `xissimarfgen`. We generated the first Ancillary Response File (ARF) by feeding an image, constructed from the double β model fit to the *Chandra* surface brightness profile, into `xissimarfgen`. This ARF was later used to model the cluster emission. For the second ARF, which was used when modeling the Galactic and cosmic X-ray background, we assumed a uniform photon distribution. We simulated 10^7 photons per detector for each of the 159 energies (medium sampling).

Night Earth data were used to create spectra of the particle background for each region and each detector, weighting the spectra by cutoff rigidity.¹ These particle spectra were supplied as background spectra to the `XSPEC` (version 12.3.1) fitting routine. The cluster emission was modeled with an ab-

sorbed thermal model (`phabs*apec`). The cosmic X-ray background and Galactic emission were accounted for with an absorbed powerlaw and an unabsorbed thermal model, respectively (`phabs*pow+apec`).

All 16 spectra were fitted simultaneously. We froze the hydrogen column density at 6.07×10^{20} cm⁻² (Kalberla et al. 2005), the cluster redshift at $z = 0.1523$ (Struble & Rood 1987), the redshift and abundance of the Galactic component at $z = 0$ and $A = 1$ solar, and the powerlaw photon index at 1.41 (Kushino et al. 2002). Annulus 4 served to help constrain the background components because no significant “contaminating” cluster emission is expected beyond the estimated r_{200} , so the normalization of the thermal cluster model was frozen at 0 in this annulus.

In the spectral fitting for this hot cluster, we ignored all photons with energies ≤ 0.7 keV. We did this in order to minimize any systematic uncertainties due to the correction for the effective area degradation by the contamination, due to the Galactic background subtraction, and due to the influence of possible low intensity solar wind charge exchange emission. The upper energy range used for the fitting was set at 10 keV (8 keV for XIS-1, due to remaining calibration uncertainties). The Si K edge (1.8–1.9 keV) and, for XIS-0, the calibration Mn K line (5.7–6.0 keV) were excluded. The range 7.2–8.0 keV was ignored because of the presence of the strong instrumental Ni K line. Overall, the model provided a good description of the data, resulting in $\chi_{\text{red}}^2 = 1.20$ for 4097 degrees of freedom.

3. Results

Figure 1 (right) shows projected gas temperature profiles measured with *Chandra*, *XMM-Newton*, and *Suzaku*. In the innermost region ($\lesssim 0.4'$) the *XMM-Newton* temperature is consistent with the range of best fit temperatures obtained with *Chandra* (3.5–7.6 keV). In the region ~ 1 – $2'$, however, *Chandra* gives systematically higher temperatures than *XMM-Newton*. The primary reasons for this are, first, that the *XMM-Newton* profile is not corrected for PSF smearing, so the temperatures in this region are slightly underestimated; and, second, that the *Chandra* effective area calibration is, apparently, inaccurate, resulting in overestimates of the temperature at high temperatures (e.g., Snowden et al. 2008; Sun et al. 2008, and L. David’s presentation²). The central *Chandra* temperatures determined here are consistent with those from Sanders et al. (2005). In the region ~ 3 – $6'$ *Chandra* and *XMM-Newton* give consistent results.

The *Suzaku* best fit temperatures and uncertainties are given in Tab. 1. The innermost *Suzaku* bin covers 0– $3.5'$ and, obviously, contains emission from quite a range of temperatures. The result of the single temperature fit lies roughly in the middle of this temperature range, as expected. The *Suzaku* best fit temperature in the second bin (3.5 – $7.5'$) is slightly higher compared to the *Chandra* and *XMM-Newton* temperatures. The primary reason for this is most likely contamination from emission from the very bright region $< 3.5'$ due to *Suzaku*’s PSF (contamination is $\sim 50\%$, see discussion below). Even though A2204 appears quite regular on large scales (e.g., Schuecker et al. 2001), possible deviations from exact spherical symmetry of the temperature structure may also introduce some scatter in the comparisons.

For the purpose of this Letter, bin 3 covers the most important region. It extends from 7.5 to $11.5'$; i.e., from 64% to 98% of the estimated r_{200} . The *Suzaku* best fit temperature ($4.49^{+0.79}_{-0.59}$

¹ See <http://www.astro.isas.jaxa.jp/suzaku/analysis/xis/nte/> for details. Additionally, we discarded a very small fraction of events by requiring `T_SAA_HXD>436`, resulting in 795 ks total exposure time.

² http://cxc.harvard.edu/ccw/proceedings/07_proc/presentations/david/

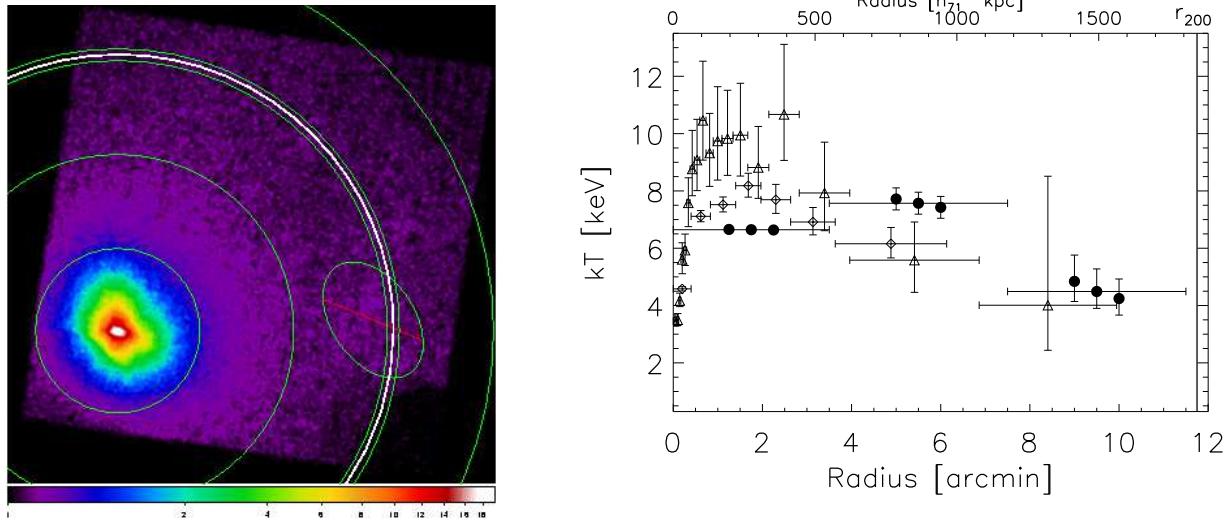


Fig. 1. *Left panel:* *Suzaku* image of A2204 combining all four XIS detectors. Also indicated are the regions used for the spectral analysis (green) and the estimated r_{200} (white). The outermost annulus (annulus 4, beyond r_{200}) was used to aid in the local background estimation. The elliptical region contains emission from unrelated sources and was excluded from the spectral analysis. *Right panel:* Gas temperatures as function of radius as measured with *Suzaku* (filled circles), *XMM-Newton* (diamonds), and *Chandra* (triangles). For each *Suzaku* bin three temperatures are shown. The upper and lower temperature values were obtained by artificially decreasing and increasing the particle background normalization by 10%, respectively. The bins are slightly offset in this plot for clarity. All errors are given at the 90% confidence level.

Table 1. Best fit *Suzaku* cluster temperatures and uncertainties (90% confidence level) of the three radial bins.

Radius/[']	kT_X /[keV]
0–3.5	$6.65^{+0.08}_{-0.08}$
3.5–7.5	$7.57^{+0.39}_{-0.38}$
7.5–11.5	$4.49^{+0.79}_{-0.59}$

keV) is significantly lower than the temperatures measured further in. For *Chandra* and *XMM-Newton*, temperature measurements in the low surface brightness cluster outskirts are strongly affected by the uncertainty in the particle background. We tested the influence of the particle background on the *Suzaku* results by artificially changing the normalization of the Night Earth spectra by a very conservative (e.g., Tawa et al. 2008) $\pm 10\%$ and repeating the fitting procedure. We found that the new best fit temperatures are consistent with the statistical uncertainty of the standard fit (Fig. 1). This demonstrates that the results obtained here are not affected significantly by uncertainties in the particle background subtraction.

We also attempted a temperature measurement with *Chandra* in the region 6.9–9.9'. The *Chandra* best fit temperature is consistent with the allowed *Suzaku* temperature range but the statistical uncertainty (excluding systematic effects due to the particle background) is too large for a meaningful constraint of the temperature with *Chandra*.

4. Discussion

We showed clear evidence that in the very outermost region of this relaxed cluster, the gas temperature drops significantly. This is expected theoretically (e.g., Frenk et al. 1999). To compare, in detail, the result obtained here to predictions, we overplotted in

Fig. 2 (left) the average temperature profile in cluster outskirts as determined with hydrodynamical simulations of massive clusters by Roncarelli et al. (2006, Sample A in their Tab. 2). These authors specifically studied the regions around the virial radius. Note that magnetic fields and cosmic rays were not included in their simulations. For the comparison, we used $r_{200} = 11.75'$ and $kT_X(0.3r_{200}) = 7.42$ keV. The latter was calculated by taking the average of the best fit *Chandra* and *XMM-Newton* temperatures of the bins that include $0.3r_{200}$ (shown in Fig. 2, left). We excluded the *Suzaku* measurement because its broad PSF makes an accurate determination at this radius difficult.

The temperature of the inner *Suzaku* bin shown is slightly higher but consistent with the prediction (keep in mind that, in general, regions left of bin centers carry more weight in the temperature determination than regions right of bin centers, because the surface brightness decreases rapidly with radius). As mentioned above and discussed in more detail below, this bin is strongly affected by PSF smearing, so the actual projected temperature may be lower. Due to the steep surface brightness profile, deprojection would likely result in only a minor increase of the temperature estimate. The important outer bin is much less affected by PSF and projection effects and is slightly lower but consistent with the prediction. In conclusion, the observed outer temperature profile is slightly steeper but consistent with a drop of a factor of 0.6 from $0.3 r_{200}$ to r_{200} , as predicted by simulations. This is the primary conclusion of this Letter. Below, we discuss possible systematic effects, finding no strong indication for a significant bias.

We showed above that uncertainties in the particle background do not affect this conclusion. Now, we discuss the influence of *Suzaku*'s PSF. We performed ray tracing simulations using the xissim tool (Ishisaki et al. 2007) using 10^7 photons per energy and detector. We assumed Abell 2204's surface brightness profile to follow the best double β model fit to the *Chandra* data. We followed a procedure very similar to the one described by Sato et al. (2007) and found that the inner bin (3.5–7.5') is

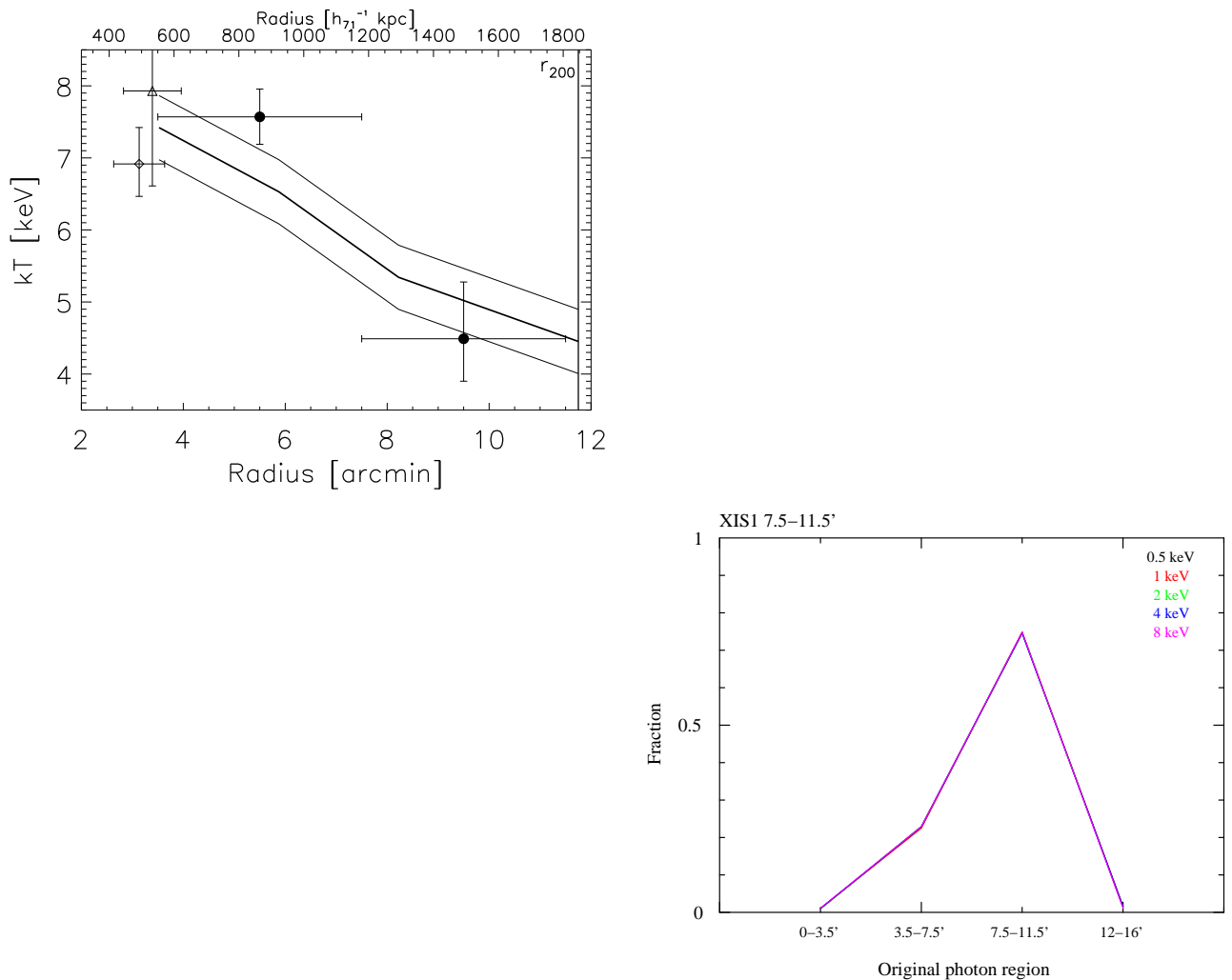


Fig. 2. *Left panel:* Observed outer temperature profile (symbols have the same meaning as in Fig. 1) compared to profile and scatter predicted by hydrodynamical simulations of Roncarelli et al. (2006, solid lines). *Right panel:* Contamination fractions of the XIS1 bin 7.5–11.5' determined from ray tracing simulations. 75% of the photons detected in this bin also originated in this region. The energy dependence is negligible (the lines for all five energies overlap) and the results are very similar for the other detectors.

significantly (49%) contaminated by emission originating in the cluster center ($<3.5'$). The most important region, the outer bin (7.5–11.5') is contaminated by 25%; i.e., a relatively small fraction (see Fig. 2, right, for the contamination fractions of this bin determined for XIS1, as a representative example). The energy and detector dependence of the PSF was found to be small enough to be negligible here. The same is true for the fine details of the model for the surface brightness profile, since we found very similar fractions when repeating this analysis using the best fit double β model as obtained from *ROSAT* *PSPC* pointed data.

Naively, one could assume that a simple PSF contamination correction could be performed, starting with the assumption that 49% of the emission in the 3.5–7.5' bin comes from a plasma at $kT_X = 4.49$ keV (Tab. 1). However, this would not be accurate, as the *Chandra* and *XMM-Newton* data reveal a large range of temperatures at different distances from the cluster center (Fig. 1). A detailed correction for the PSF effects, therefore, requires a large number of ray tracing simulations to be performed, using fine *Chandra* temperature bins, in order to determine precisely how much emission from plasma at what temperature contaminates each of the *Suzaku* bins. This is beyond the scope of this Letter. Such a correction will be performed in a more in-depth

analysis, after the next *Chandra* effective area calibration update has been released, using the longer *Chandra* observation of this cluster that will become publically available soon. However, it is expected that the *Suzaku* temperature in the bin that goes out to r_{200} will not change dramatically due to such a correction, since we showed that the contamination is relatively small in any case. A possible slight change would likely decrease the temperature somewhat, because all the plasma at inner radii (responsible for the contamination) has higher temperatures, and our conclusion of a detection of a significant temperature drop in the outskirts would be further strengthened.

We specifically designed the *Suzaku* observation in such a way as to have a cluster free region available to help constrain Galactic and cosmic X-ray background directly and locally, using the same observation. This ensures that the results are not affected by systematic calibration differences between different satellites and varying point source subtraction fractions. Still, we checked whether the resulting parameter values are in a reasonable range. We found that the normalization of the power law component expected from deep CXB studies using several different satellites is lower by factors 0.77–0.62 compared to our best fit normalization. We then froze the powerlaw normalization

to the highest (Vecchi et al. 1999) and lowest (Revnivtsev et al. 2003) normalization we found in the literature, resulting in temperatures $6.08^{+0.98}_{-0.82}$ and $6.84^{+1.17}_{-0.72}$ keV, respectively, in the outer bin. This procedure results in worse fits but note that, in the latter case, the temperature is significantly hotter than when leaving the powerlaw normalization free. Since intensity variations of the CXB may be correlated with large scale structure, we decided to use the independent *ROSAT* *PSPC* observation of Abell 2204 and fitted the same background model in the energy band 0.3–2.4 keV to the outskirts. We found that the normalization is fully consistent (factor 0.81–1.04) with the higher powerlaw normalization from the *Suzaku* data of Abell 2204. Moreover, we also found the temperature and normalization of the thermal component to be fully consistent with the *Suzaku* results. In particular, for the Galactic emission, we found temperatures of $0.25^{+0.02}_{-0.01}$ keV (*Suzaku*) and $0.26^{+0.01}_{-0.01}$ keV (*ROSAT*), quite typical for this background component; i.e., there was no indication of significant hot cluster or accretion shock emission “contaminating” annulus 4. We, therefore, conclude that our Galactic and cosmic background modeling is adequate. In any case, a possible slight increase of the outermost temperature due to overestimated powerlaw intensity would result in even better agreement with the simulation results.

For the comparison to simulated temperature profiles, the uncertainty of r_{200} as estimated from the extrapolated *XMM-Newton* density and temperature profiles may be important. For instance, using a cluster mean temperature and the relation of Evrard et al. (1996) would result in a larger value for r_{200} . This would make the observed temperature drop even steeper in terms of r_{200} , potentially resulting in tension between observation and simulations. We will redetermine r_{200} from the cluster mass profile, taking advantage of the information on the outer temperature from *Suzaku* in the more in-depth analysis of this cluster. It is reassuring to note that further corroboration for the r_{200} estimate used here comes from the independent weak lensing analysis of this cluster (Clowe & Schneider 2002), yielding $r_{200} = 11.8'$, in perfect agreement with our estimate.

The confirmation of the predictions from hydrodynamical simulations for the gas physics in cluster outskirts indicated here rests on the analysis of a single cluster. What is required for a general confirmation is the analysis of a statistical sample of clusters. In the future, this can be performed with cluster data accumulating rapidly in the *Suzaku* archive. As a first step, we obtained/will obtain *Suzaku* data for two more *HIFLUGCS* clusters, A2244 and A2163, which we will use for very similar measurements.

Acknowledgements. THR acknowledges the hospitality of Tokyo Metropolitan University. We thank T. Erben, G. Hasinger, O.-E. Nenyshyan, and P. Schneider for help in the early stages of this work. THR, DSH, YYZ acknowledge support by the Deutsche Forschungsgemeinschaft through Emmy Noether Research Grant RE 1462 and by the German BMBF through the Verbundforschung under grant no. 50 OR 0601. KS acknowledges support by the Ministry of Education, Culture, Sports, Science and Technology of Japan, Grant-in-Aid for Scientific Research No. 19840043. NO thanks the Alexander von Humboldt Foundation for support.

References

- Allen, S. W., Schmidt, R. W., & Fabian, A. C. 2001, *MNRAS*, 328, L37
- Arnaud, M., Pointecouteau, E., & Pratt, G. W. 2005, *A&A*, 441, 893
- Clowe, D. & Schneider, P. 2002, *A&A*, 395, 385
- De Grandi, S. & Molendi, S. 2002, *ApJ*, 567, 163
- Evrard, A. E., Metzler, C. A., & Navarro, J. F. 1996, *ApJ*, 469, 494
- Frenk, C. S., White, S. D. M., Bode, P., et al. 1999, *ApJ*, 525, 554
- Fujimoto, R., Mitsuda, K., Mccammon, D., et al. 2007, *PASJ*, 59, 133
- Fujita, Y., Tawa, N., Hayashida, K., et al. 2008, *PASJ*, 60, S343
- Fukazawa, Y. 1997, PhD thesis, Univ. Tokyo
- Hudson, D. S. & Reiprich, T. H. 2006, in *Heating vs. Cooling in Galaxies and Clusters of Galaxies*, ed. H. Böhringer, P. Schuecker, G. W. Pratt, & A. Finoguenov (Berlin, Germany: ESO Astrophysics Symposia, Springer Verlag)
- Hudson, D. S., Reiprich, T. H., Clarke, T. E., & Sarazin, C. L. 2006, *A&A*, 453, 433
- Irwin, J. A. & Bregman, J. N. 2000, *ApJ*, 538, 543
- Irwin, J. A., Bregman, J. N., & Evrard, A. E. 1999, *ApJ*, 519, 518
- Ishisaki, Y., Maeda, Y., Fujimoto, R., et al. 2007, *PASJ*, 59, 113
- Kalberla, P. M. W., Burton, W. B., Hartmann, D., et al. 2005, *A&A*, 440, 775, http://www.astro.uni-bonn.de/~webraai/english/tools_labsurvey.php
- Kotov, O. & Vikhlinin, A. 2005, *ApJ*, 633, 781
- Kushino, A., Ishisaki, Y., Morita, U., et al. 2002, *PASJ*, 54, 327
- Leccardi, A. & Molendi, S. 2008, *A&A*, accepted. Preprint: arXiv:0804.1909
- Markevitch, M., Forman, W. R., Sarazin, C. L., & Vikhlinin, A. 1998, *ApJ*, 503, 77
- Mitsuda, K., Bautz, M., Inoue, H., et al. 2007, *PASJ*, 59, 1
- Piffaretti, R., Jetzer, P., Kaastra, J. S., & Tamura, T. 2005, *A&A*, 433, 101
- Pratt, G. W., Böhringer, H., Croston, J. H., et al. 2007, *A&A*, 461, 71
- Reiprich, T. H. & Böhringer, H. 2002, *ApJ*, 567, 716
- Revnivtsev, M., Gilfanov, M., Sunyaev, R., Jahoda, K., & Markwardt, C. 2003, *A&A*, 411, 329
- Roncarelli, M., Ettori, S., Dolag, K., et al. 2006, *MNRAS*, 373, 1339
- Sanders, J. S., Fabian, A. C., & Taylor, G. B. 2005, *MNRAS*, 356, 1022
- Sato, K., Yamasaki, N. Y., Ishida, M., et al. 2007, *PASJ*, 59, 299
- Schuecker, P., Böhringer, H., Reiprich, T. H., & Feretti, L. 2001, *A&A*, 378, 408
- Snowden, S. L., Mushotzky, R. F., Kuntz, K. D., & Davis, D. S. 2008, *A&A*, 478, 615
- Solovyeva, L., Anokhin, S., Sauvageot, J. L., Teyssier, R., & Neumann, D. 2007, *A&A*, 476, 63
- Struble, M. F. & Rood, H. J. 1987, *ApJS*, 63, 543
- Sun, M., Voit, G. M., Donahue, M., Jones, C., & Forman, W. 2008, *ApJ*, submitted. Preprint: arXiv:0805.2320, 805
- Tawa, N., Hayashida, K., Nagai, M., et al. 2008, *PASJ*, 60, S11
- Vecchi, A., Molendi, S., Guainazzi, M., Fiore, F., & Parmar, A. N. 1999, *A&A*, 349, L73
- Vikhlinin, A., Markevitch, M., Murray, S. S., et al. 2005, *ApJ*, 628, 655
- White, D. A. 2000, *MNRAS*, 312, 663
- Zhang, Y.-Y., Finoguenov, A., Böhringer, H., et al. 2004, *A&A*, 413, 49
- Zhang, Y.-Y., Finoguenov, A., Böhringer, H., et al. 2008, *A&A*, 482, 451